# Spectral function of a single hole in a two-dimensional quantum antiferromagnet

Frank Marsiglio*
*Department of Physics, University of California at San Diego, La Jolla, California 92093*

Andrei E. Ruckenstein
*Serin Physics Laboratory, Rutgers University, Piscataway, New Jersey 08855*

Stefan Schmitt-Rink and Chandra M. Varma
*AT&T Bell Laboratories, Murray Hill, New Jersey 07974*
(Received 21 September 1990)

The spectral function of a single hole moving in a two-dimensional antiferromagnetic background is calculated, using the self-consistent Born approximation for the self-energy. For small systems, good agreement is found with the results of exact diagonalization studies. In the thermodynamic limit, the quasiparticle residue, the effective mass, and the incoherent multiple spin-wave background are determined as functions of the ratio of Heisenberg exchange $J$ and hopping amplitude $t$. The relevance of the single-hole results to the physical problem of a finite hole concentration is briefly discussed.

## I. INTRODUCTION

In a recent letter, a simple method was proposed to calculate the spectral function of a single hole in an $S=\frac{1}{2}$ Heisenberg quantum antiferromagnet (QAFM).[1] The method exploited the formal similarity of the QAFM problem to that of superfluid $^4$He and the motion of a hole in the former to the motion of a defect (a $^3$He atom) in the latter, a problem discussed in a classic paper by McMillan.[2] The method is also related to the work of Lee, Low, and Pines and others on the motion of an electron in a polar crystal.[3]

For illustrative purposes, only the results for the spectral function of a single hole in one dimension (1D) were presented.[1] The results do depend on the dimensionality, and so we present here detailed numerical studies of the two-dimensional (2D) case. In particular, we calculate the "quasiparticle" residue $z_{\mathbf{k}}$ and effective mass $m^*$ at the bottom of the band as functions of the ratio of Heisenberg exchange $J$ and hopping amplitude $t$. Kane, Lee, and Read have made analytical approximations to the form of the spectral function given in Ref. 1 to evaluate these quantities.[4] Except for extremely small values of $J/t$, our results for $z_{\mathbf{k}}$ and $m^*$ do not agree with theirs. Recently, the spectral function for small lattices has been calculated exactly.[5,6] Our results compare very well with these.

Spurred by the discovery of high-temperature superconductivity in $CuO_2$-based materials, which at "half-filling" are antiferromagnetic insulators well described by the Heisenberg model, there have been numerous other papers on the motion of a single hole in a QAFM (see, for example, Refs. 7-13). We will not comment on these, except insofar as they involve the approximate scheme introduced in Ref. 1.

Since the undoped $CuO_2$-based materials are charge transfer insulators, we do not believe that the model under consideration is sufficient to describe the metallic phase of high-temperature superconductors. The question which we will briefly discuss here is the relevance of the single-hole problem within the doped Heisenberg (or Hubbard) model to the transition from the insulating antiferromagnetic phase to the metallic nonmagnetic phase.

## II. EFFECTIVE HAMILTONIAN FOR A SINGLE HOLE

Consider the Neel state $|N\rangle$ as the vacuum state, and define hole operators $h_i$ such that $h_i=c_{i\uparrow}^\dagger$ on the $\uparrow$ sublattice and $c_{i\downarrow}^\dagger$ on the $\downarrow$ sublattice. Also define spin-flip operators $b_i=c_{i\uparrow}^\dagger c_{i\downarrow}$ on the $\uparrow$ sublattice and $c_{i\downarrow}^\dagger c_{i\uparrow}$ on the $\downarrow$ sublattice. Thus, $b_i|N\rangle=0$ and $b_i^\dagger=S_i^-$ on the $\uparrow$ sublattice and $S_i^+$ on the $\downarrow$ sublattice. The $h$'s obey Fermi statistics and the $b$'s hard-core boson commutation rules.

With these definitions, one can write down the following Hamiltonian for the motion of a hole in a QAFM[1]

$$H_t=t\sum_{\langle i,j\rangle} h_i^\dagger h_j[b_j^\dagger(1-b_i^\dagger b_i)+(1-b_j^\dagger b_j)b_i]\ . \tag{1}$$

$H_t$ properly describes the change in spin configuration due to this motion. Consider, for instance, $H_t h_j^\dagger|N\rangle=b_j^\dagger h_i^\dagger|N\rangle$, which shows the correct alteration in the spin configuration of the Neel state due to the hopping of a hole from site $j$ to site $i$. In addition, $H_t$ commutes with the number of doubly occupied sites $\sum_i h_i^\dagger h_i b_i^\dagger b_i$ and thus preserves the constraint of no double occupancy.

The Heisenberg exchange Hamiltonian $H_J$ may similarly be written in terms of $b$'s and projection operators $1-h_i^\dagger h_i$. In this paper, we ignore the latter as well as the factors $1-b_i^\dagger b_i$ in Eq. (1), i.e., the hard-core constraints (see below). Within linear spin-wave theory (i.e., treating the $b$'s as ideal bosons), $H_t$ and $H_J$ then reduce to

 

$$H_t = t \sum_{\langle i,j \rangle} h_i^\dagger h_j (b_j^\dagger + b_i) , \tag{2a}$$

$$H_J = \frac{J}{2} \sum_{\langle i,j \rangle} (2 b_i^\dagger b_i + b_i b_j + b_j^\dagger b_i^\dagger) - \frac{NJz}{4} . \tag{2b}$$

Here, $z$ is the coordination number of the lattice. Equations (2) are rewritten in momentum space as

$$H_t = \frac{tz}{N^{1/2}} \sum_{\mathbf{k},\mathbf{q}} h_{\mathbf{k}}^\dagger h_{\mathbf{k}-\mathbf{q}} (\gamma_{\mathbf{k}} b_{-\mathbf{q}}^\dagger + \gamma_{\mathbf{k}-\mathbf{q}} b_{\mathbf{q}}) , \tag{3a}$$

$$H_J = \frac{Jz}{2} \sum_{\mathbf{k}} [2 b_{\mathbf{k}}^\dagger b_{\mathbf{k}} + \gamma_{\mathbf{k}} (b_{\mathbf{k}} b_{-\mathbf{k}} + b_{-\mathbf{k}}^\dagger b_{\mathbf{k}}^\dagger)] - \frac{NJz}{4} , \tag{3b}$$

where $\gamma_{\mathbf{k}} = \sum_\delta \exp(i\mathbf{k}\cdot\delta)/z$, $\delta$ being a nearest-neighbor vector.

$H_J$ can be diagonalized by using the Bogoliubov transformation $b_{\mathbf{k}} = u_{\mathbf{k}} a_{\mathbf{k}} + v_{\mathbf{k}} a_{-\mathbf{k}}^\dagger$, where

$$u_{\mathbf{k}} = \{ \tfrac{1}{2} [ (1-\gamma_{\mathbf{k}}^2)^{-1/2} + 1 ] \}^{1/2} , \tag{4a}$$

$$v_{\mathbf{k}} = -\mathrm{sgn}(\gamma_{\mathbf{k}}) \{ \tfrac{1}{2} [ (1-\gamma_{\mathbf{k}}^2)^{-1/2} - 1 ] \}^{1/2} . \tag{4b}$$

This gives[1]

$$H_t = \frac{tz}{N^{1/2}} \sum_{\mathbf{k},\mathbf{q}} h_{\mathbf{k}}^\dagger h_{\mathbf{k}-\mathbf{q}} [ (\gamma_{\mathbf{k}} u_{\mathbf{q}} + \gamma_{\mathbf{k}-\mathbf{q}} v_{\mathbf{q}}) a_{-\mathbf{q}}^\dagger + (\gamma_{\mathbf{k}} v_{\mathbf{q}} + \gamma_{\mathbf{k}-\mathbf{q}} u_{\mathbf{q}}) a_{\mathbf{q}} ] , \tag{5a}$$

$$H_J = \sum_{\mathbf{k}} \omega_{\mathbf{k}} (a_{\mathbf{k}}^\dagger a_{\mathbf{k}} + \tfrac{1}{2}) - \frac{3NJz}{4} , \tag{5b}$$

where $\omega_{\mathbf{k}} = Jz(1-\gamma_{\mathbf{k}}^2)^{1/2}$ is the spin-wave dispersion. Identical expressions for $H_t$ and $H_J$ have been derived in Ref. 4 starting from a Schwinger boson representation.

It is worth bearing in mind the physical approximation underlying the above linear spin-wave theory. The ground-state wave function of $H_J$ is simply

$$|0\rangle = \exp\left[ - \sum_{\mathbf{k}>0} \lambda_{\mathbf{k}} b_{\mathbf{k}}^\dagger b_{-\mathbf{k}}^\dagger \right] |N\rangle = \exp\left[ - \sum_{i<j} \lambda_{ij} b_i^\dagger b_j^\dagger \right] |N\rangle , \tag{6}$$

with $\lambda_{\mathbf{k}} = -v_{\mathbf{k}}/u_{\mathbf{k}}$, and describes the best possible harmonic approximation to the full QAFM problem. $|0\rangle$ includes (in an approximate fashion) the zero-point spin deviations, but violates the hard-core constraint. The long-wavelength behavior and therefore the asymptotic power-law decay of spin deviations are well described, since they are determined by the linear dispersion of spin waves $\omega_{\mathbf{k}} \sim k$ at small $k$ which, itself, follows from symmetries alone. An adequate description of the short-wavelength behavior, however, requires a correct treatment of the hard-core constraint. This can be done as in Feynman's classic work on $^4$He,[14] by considering a Jastrow-like wave function, which is obtained by expanding the exponential in Eq. (6) and keeping only the first two terms [since the rest are eliminated by the hard-core condition $(b_i^\dagger)^2 = 0$],

$$|0\rangle = \prod_{i<j} (1 - \lambda'_{ij} b_i^\dagger b_j^\dagger) |N\rangle . \tag{7}$$

$\lambda'_{\mathbf{k}}$, the Fourier transform of $\lambda'_{ij}$, can be related to the susceptibility $\chi(\mathbf{k})$, just as the analogous quantity in the $^4$He problem was related by Feynman to the structure factor $S(\mathbf{k})$.[14] $\lambda'_{\mathbf{k}}$ at long wavelengths is determined by the spin-wave frequencies, just as $\lambda_{\mathbf{k}}$ in Eq. (6). Ground- and excited-state wave functions of $H_J$ in the presence of a static hole can be similarly defined and, in analogy with McMillan's work on the motion of $^3$He atoms in superfluid $^4$He,[2] matrix elements of $H_t$ in this basis set can be calculated. The evaluation of these quantities entails extensive numerical calculations, which we have not pursued. We have satisfied ourselves, however, that the qualitative behavior so obtained is not different from the results obtained here ignoring the hard-core constraints. Wave functions of the form Eq. (7) have been considered, for example, by Bartkowski[15] and Sachdev.[11]

## III. SPECTRAL FUNCTION OF A SINGLE HOLE

Given the matrix elements (5a) for spin-wave absorption and emission, the self-energy of a hole in the self-consistent Born ("noncrossing") approximation is[1]

$$\Sigma(\mathbf{k},\omega) = \frac{t^2 z^2}{N} \sum_{\mathbf{q}} (u_{\mathbf{q}} \gamma_{\mathbf{k}-\mathbf{q}} + v_{\mathbf{q}} \gamma_{\mathbf{k}})^2 G(\mathbf{k}-\mathbf{q}, \omega - \omega_{\mathbf{q}}) , \tag{8}$$

where

$$G(\mathbf{k},\omega) = [\omega - \Sigma(\mathbf{k},\omega) + i0]^{-1} \tag{9}$$

is the hole Green's function. The spectral function as usual is

$$A(\mathbf{k},\omega) = -\frac{1}{\pi} \mathrm{Im} G(\mathbf{k},\omega) . \tag{10}$$

In two and higher dimensions, $A(\mathbf{k},\omega)$ displays a narrow peak as a function of $\omega$ for a given $\mathbf{k}$, i.e., a "quasiparticle" part, and a broad incoherent background which reflects real multiple spin-wave processes accompanying hole motion.[1,4] The quasiparticle part, which reflects Bloch-like propagating motion, is absent for hole motion in an Ising model for which the ground state is the Neel state.[7-9] In the QAFM, the ground state is a linear combination of the Neel state and states with multiple zero-point spin deviations. As the hole hops, it also creates spin deviations. The spin configuration after a hop has a finite overlap with the spin configuration prior to the hop, hence a Bloch-like propagation. The quasiparticle spectral weight is proportional to this overlap. Below, we will present an evaluation of this quantity and the quasiparticle dispersion $\varepsilon_{\mathbf{k}}$. Note from Eqs. (8) and (9) that $G(\mathbf{k},\omega) = G(\mathbf{k}+\mathbf{Q},\omega)$, where $\mathbf{Q} = (\pi,\pi,\ldots)$ is the wave vector of the antiferromagnetic spin-density wave. The dispersion of $\varepsilon_{\mathbf{k}}$ is thus, like that of next-nearest-neighbor hopping, as expected for a hypercubic lattice with sublattice magnetization.

The self-energy Eq. (8) ignores vertex corrections. For $J \gg t$, where perturbation theory in $t/J$ becomes valid, this approximation is rigorously justified (see below).[1] In the opposite limit, $J \ll t$, the vertex has to be of order $t$, as in Eq. (8). Vertex corrections, therefore, are unlikely

to introduce a new energy scale and thus are not expected to change the results qualitatively. This view is supported by the good agreement of our results with exact diagonalization studies.

It is worth noting that the hole wave function within our simple approximation has the form of a moving particle dressed by backflow of spin waves. At long distances, the form of the spin distortion is dipolar. This can be seen by expanding the scattering matrix element in Eq. (8) for small $\mathbf{q}$: $u_q\gamma_{k-q}+v_q\gamma_k \sim v_k\cdot q/q^{1/2}$, where $\mathbf{v_k}=\nabla_k\gamma_k$ is the velocity. Thus, the admixture of a spin distortion with wave vector $\mathbf{q}$ in the wave function has a coefficient $\mathbf{v_k}\cdot\mathbf{q}/q^2$ exhibiting dipolar backflow. This is exactly as for a moving $^3$He atom[2] or a roton[14] in superfluid $^4$He. In the context of the present problem, this dipolar distortion has also been discussed by Shraiman and Siggia, using more sophisticated arguments.[9]

## IV. NUMERICAL RESULTS

Equations (8) and (9) can be solved numerically by iteration on a discrete mesh of $\mathbf{k}$ and $\omega$ points.[1] Due to the symmetries of $G(\mathbf{k},\omega)$, the calculation can be limited to the irreducible part of the Brillouin zone shown in Fig. 1 (shaded wedge). An artificial broadening parameter $\Delta\omega \ll t$ is introduced in Eq. (9), to make the iteration procedure stable. For certain parameters, it is necessary to step $\Delta\omega$ down gradually to its final value.

We first solved Eqs. (8) and (9) for a $4\times4$ lattice, which has been studied extensively by exact diagonalization.[5,6] This allows us to assess the quality of the approximations made. Figure 2 shows the hole spectral function $A(\mathbf{k},\omega)$ at $\mathbf{k}=\mathbf{Q}/2=(\pi/2,\pi/2)$ for (a) $J=0$, (b) $J=0.2t$, and (c) $J=0.7t$. This value of $\mathbf{k}$ corresponds to the hole ground state, at least for cases (b) and (c). (For very small values of $J/t$, the system ground state is a saturated ferromagnet.[16]) As already mentioned, the spectra display a pronounced low-energy peak which is the quasiparticle peak predicted in Refs. 1 and 4. With decreasing $J$, this peak moves to lower energies and its weight decreases, as expected. The missing spectral weight appears in the form of incoherent real multiple spin-wave excitations at higher energies. The total spectral weight is of course conserved and equal to 1.

The spectra shown in Fig. 2 are in good agreement with the exact diagonalization results of Refs. 5 and 6 (their Figs. 5 and 10, respectively) and qualitatively similar to those reported in Ref. 1 for one dimension. For $J=0$ [Fig. 2(a)], the spectrum is completely incoherent, extending over almost the full free-hole bandwidth $8t$. It is furthermore symmetric about $\omega=0$,with a "gap" in the middle. (As shown below, this gap is a finite-size effect and disappears in the thermodynamic limit.) For $J=0.2t$ [Fig. 2(b)], there is a pronounced quasiparticle peak centered just below $\omega=-2t$, separated by a gap from an incoherent spectrum. Even the fine structure of the incoherent part follows the exact results, with two peaks [peaks II and III in Fig. 5(e) of Ref. 5] appearing just above the gap, followed by another gap and further incoherent excitations. For $J=0.7t$ [Fig. 2(c)], the quasiparticle peak starts to become the dominant feature, followed again by two pronounced incoherent peaks, in good agreement with the exact diagonalization results. All features—quasiparticle peaks, gaps, and incoherent real multiple spin-wave excitations—are closely reproduced by our calculation.

As expected, a detailed quantitative comparison with the exact results reveals some discrepancies. For example, Fig. 3 displays the hole ground-state energy

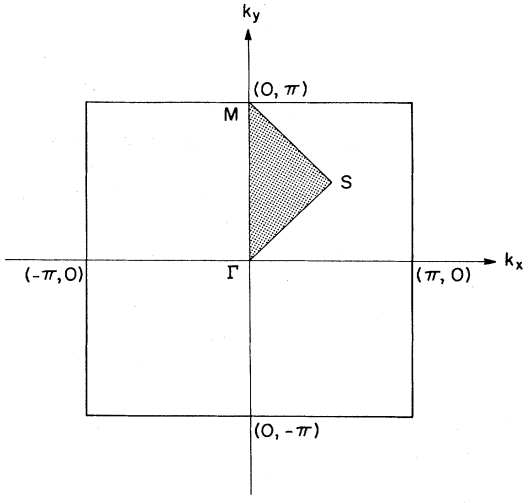


FIG. 1. Brillouin zone for a 2D square lattice. The shaded wedge marks the irreducible part which can be extended to the rest of the zone by using symmetry operations.

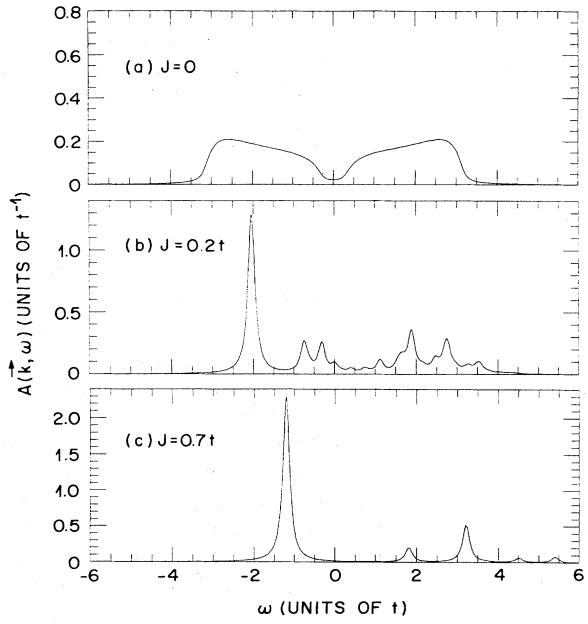


FIG. 2. Hole spectral function at $\mathbf{k}=(\pi/2,\pi/2)$ for a $4\times4$ lattice: (a) $J=0$, (b) $J=0.2t$, and (c) $J=0.7t$. The spectra are in excellent agreement with the exact diagonalization results of Refs. 5 and 6 (their Figs. 5 and 10, respectively).

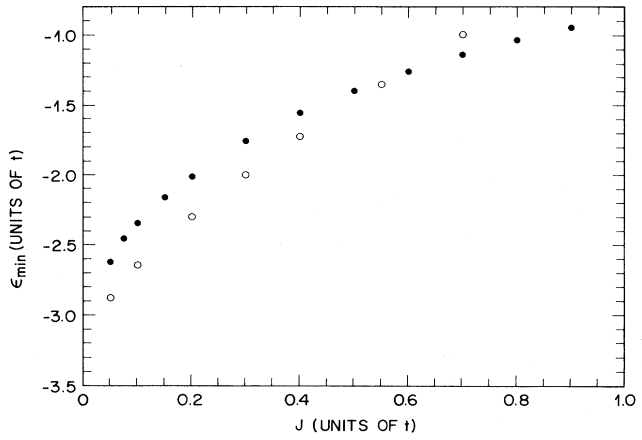


FIG. 3. Hole ground-state energy $\varepsilon_{\min}=\varepsilon(\pi/2,\pi/2)$ for a $4\times4$ lattice vs $J$ (solid circles). Open circles show the exact diagonalization results of Ref. 5.

$\varepsilon_{\min}=\varepsilon(\pi/2,\pi/2)$ versus $J$ (solid circles). The open circles show the exact diagonalization results of Dagotto *et al.*[5] which deviate somewhat from ours. Bandwidths and quasiparticle spectral weights have also been extracted from the exact diagonalization studies. We will discuss these issues below, but note in passing that for the $4\times4$ lattice $\mathbf{k}=(\pi/2,\pi/2)$, and $J<t$, we find a quasiparticle residue varying approximately like $(J/t)^{1/2}$, in agreement with Dagotto *et al.*[5] [see also Fig. 9(b)].

The influence of finite-size effects can be easily studied within our formalism, by simply increasing the system size to $20\times20$ which we found to give an adequate description of the thermodynamic limit. (In certain cases, we performed checks on sizes up to $64\times64$.) Figure 4 shows the same spectra as Fig. 2 (dashed lines), together with the corresponding hole spectral functions in the thermodynamic limit (solid lines). For $J=0$ [Fig. 4(a)], the gap in the spectrum has disappeared and the total bandwidth is somewhat larger. For $J=0.2t$ [Fig. 4(b)], the gap following the quasiparticle peak has also filled in and the two incoherent peaks just below $\omega=0$ have merged into one. In addition, there has been an overall smoothing, particularly at higher energies. The merging of the two incoherent peaks is a general finite-size effect and is more readily seen for $J=0.7t$ [Fig. 4(c)]. Simple iteration of Eq. (8) shows that these peaks derive from renormalized single spin-wave final states, with unperturbed discrete spin-wave energies $2\sqrt{3}J$ and $4J$ in the $4\times4$ system and a peak in the spin-wave density of states $4J$ in the thermodynamic limit.

The central questions in the thermodynamic limit are the dispersion and $J$ dependence of the quasiparticle energy $\varepsilon_{\mathbf{k}}$ and residue $z_{\mathbf{k}}$. Figure 5 shows the hole spectral function for $J=0.1t$ at (a) $\mathbf{k}=(\pi/2,\pi/2)$, (b) $\mathbf{k}=(0,\pi)$, (c) $\mathbf{k}=(0,0)$, and (d) $\mathbf{k}=(\pi/5,\pi/5)$. The spectra display quasiparticle peaks at all momenta and incoherent structure due to multiple spin-wave excitations. The lowest and highest energy quasiparticle states have momenta $\mathbf{k}=(\pi/2,\pi/2)$ and $\mathbf{k}=(0,0)$, respectively, and the spectral functions along $k_y=\pi-k_x$ are all very similar. The spectral weight of the quasiparticle peak decreases as one approaches the $\Gamma$ point $\mathbf{k}=(0,0)$, where it is less than 1%.

From the energetic position of the quasiparticle peak we obtain the quasiparticle dispersion $\varepsilon_{\mathbf{k}}$ shown in Fig. 6 for various values of $J$. We have plotted $(\varepsilon_{\mathbf{k}}-\varepsilon_{\min})/w$, where $w=\varepsilon(0,0)-\varepsilon_{\min}$ is the quasiparticle bandwidth.

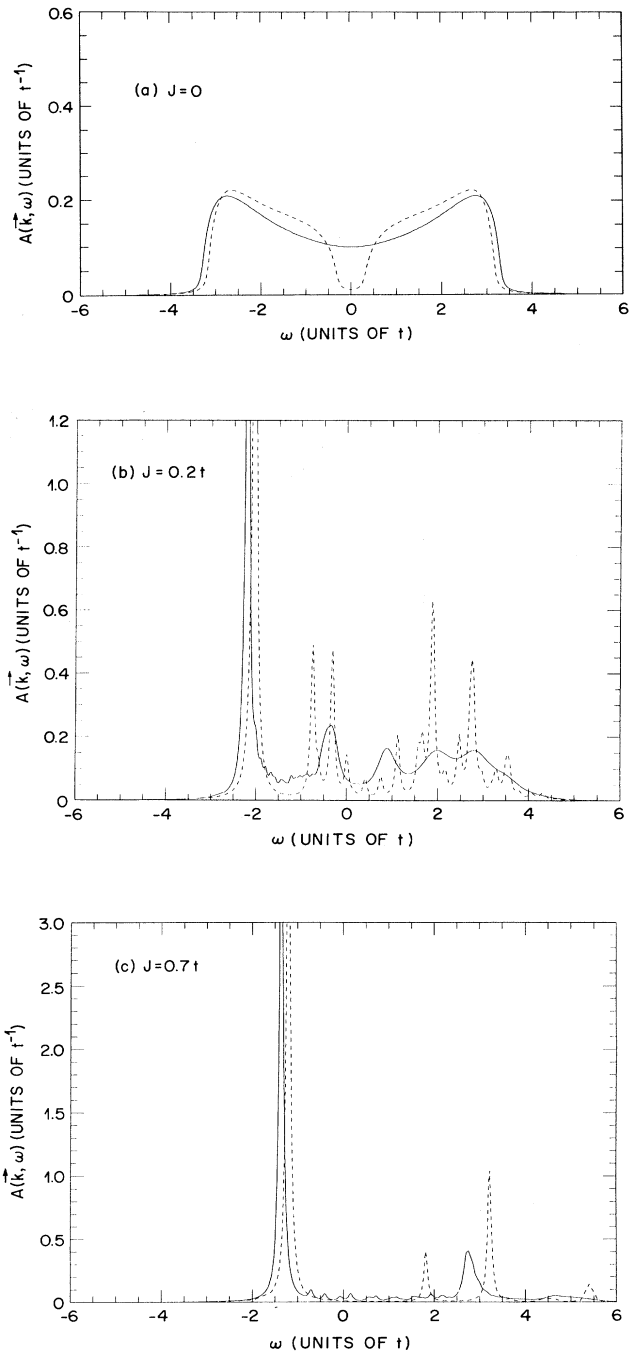


FIG. 4. Hole spectral function at $\mathbf{k}=(\pi/2,\pi/2)$ for a $4\times4$ lattice (dashed lines) and in the thermodynamic limit (solid lines): (a) $J=0$, (b) $J=0.2t$, and (c) $J=0.7t$.

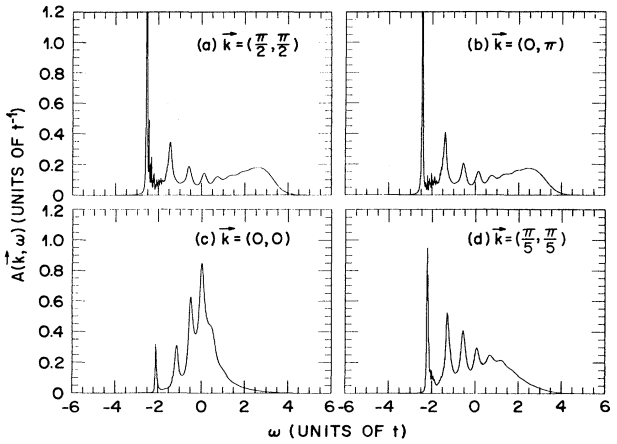


FIG. 5. Hole spectral function for $J=0.1t$: (a) $\mathbf{k}=(\pi/2,\pi/2)$, (b) $\mathbf{k}=(0,\pi)$, (c) $\mathbf{k}=(0,0)$, and (d) $\mathbf{k}=(\pi/5,\pi/5)$. The spectra in cases (a) and (b) are very similar, as are all spectra for $k_y=\pi-k_x$. At $\mathbf{k}=(0,0)$, the spectral weight of the quasiparticle peak is less than 1%. It increases as one moves away from the $\Gamma$ point.

As already noted by many authors, the effective mass along $k_y=k_x$ is much smaller than that along $k_y=\pi-k_x$ [see also Fig. 9(c)]. Von Szczepanski *et al.* have suggested the relation

$$\varepsilon_{\mathbf{k}}=\varepsilon_{\min}+(J/2)(\cos k_x+\cos k_y)^2 ,$$

consistent with next-nearest-neighbor hopping.[6] We find empirically that inclusion of further neighbors on the same sublattice through

$$\varepsilon_{\mathbf{k}}=\varepsilon_{\min}+\frac{w}{5}[(\cos k_x+\cos k_y)^2 + \tfrac{1}{4}[\cos(k_x+k_y)+\cos(k_x-k_y)]^2 \quad (11)$$

gives a reasonably good fit to the data (solid line in Fig. 6). For example, the maximum at $\mathbf{k}=(0,\pi)$ followed by the minimum near $\mathbf{k}=(0,7\pi/10)$ are reproduced by Eq. (11).

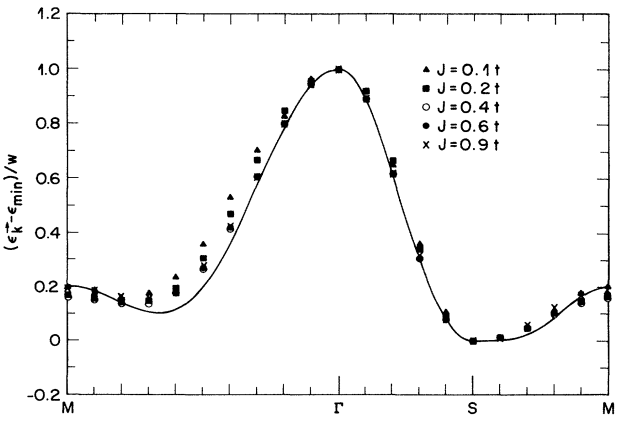


FIG. 6. Quasiparticle dispersion along the symmetry directions for various values of $J$. We have plotted $(\varepsilon_{\mathbf{k}}-\varepsilon_{\min})/w$, where $w$ is the quasiparticle bandwidth. The solid line is a fit to the data according to Eq. (11).

The quasiparticle energies in Fig. 6 have been directly obtained by solving the self-consistent equation

$$\varepsilon_{\mathbf{k}}=\mathrm{Re}\Sigma(\mathbf{k},\varepsilon_{\mathbf{k}}) . \quad (12)$$

Simultaneously, $-\mathrm{Im}\Sigma(\mathbf{k},\varepsilon_{\mathbf{k}})$ must vanish. Figure 7 shows the real (solid line) and imaginary (dashed line) parts of the hole self-energy for $J=0.2t$ at $\mathbf{k}=(\pi/2,\pi/2)$. The intersection of the straight line $\omega$ with $\mathrm{Re}\Sigma(\mathbf{k},\omega)$ yields the location of the quasiparticle pole near $\omega=-2.2t$, where $-\mathrm{Im}\Sigma(\mathbf{k},\omega)$ is infinitesimal. Immediately following this pole, $-\mathrm{Im}\Sigma(\mathbf{k},\omega)$ is quadratic in $\omega$ and then becomes of order $t$.[4] Considerable structure remains, however, and additional peaks in the spectrum [Fig. 4(b)] arise from the crossing of $\omega$ and $\mathrm{Re}\Sigma(\mathbf{k},\omega)$ at higher energies, when $-\mathrm{Im}\Sigma(\mathbf{k},\omega)$ is small.

Figure 8 shows $\varepsilon_{\mathbf{k}}$, $-\mathrm{Im}\Sigma(\mathbf{k},\varepsilon_{\mathbf{k}})$, and the quasiparticle spectral weight

$$z_{\mathbf{k}}=\left[1-\frac{\partial \mathrm{Re}\Sigma(\mathbf{k},\varepsilon_{\mathbf{k}})}{\partial\varepsilon_{\mathbf{k}}}\right]^{-1} \quad (13)$$

versus the artificial broadening $\Delta\omega$ required in the calculation. The parameters are the same as in Fig. 7. All quantities extrapolate in a linear fashion with $\Delta\omega$ towards their "intrinsic" values. The changes in $\varepsilon_{\mathbf{k}}$ and $z_{\mathbf{k}}$ are less than 1%, those in the effective mass

$$\left[\frac{1}{m^*}\right]_{ij}=\frac{\partial^2\varepsilon_{\mathbf{k}}}{\partial k_i\partial k_j} \quad (14)$$

are even smaller (not shown).

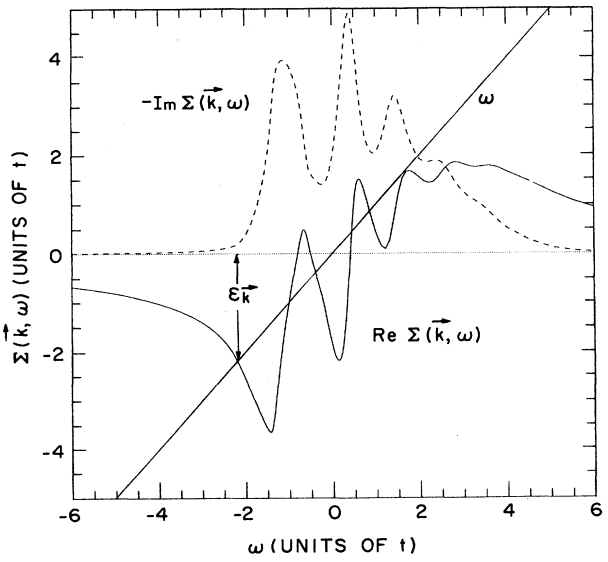


FIG. 7. Real (solid line) and imaginary (dashed line) parts of the hole self-energy for $J=0.2t$ and $\mathbf{k}=(\pi/2,\pi/2)$. The intersection near $\omega=-2.2t$ of $\mathrm{Re}\Sigma(\mathbf{k},\omega)$ with the straight line $\omega$ yields the quasiparticle energy $\varepsilon_{\mathbf{k}}$. The intersections at higher energies give rise to incoherent peaks in the spectral function, when $-\mathrm{Im}\Sigma(\mathbf{k},\omega)$ is small [see Fig. 4(b)].

Figure 9 shows (a) the hole ground-state energy $\varepsilon_{\min}$, (b) the quasiparticle residue $z(\pi/2,\pi/2)$, (c) the quasiparticle inverse effective masses $m_1^{-1}$ and $m_2^{-1}$, and (d) the quasiparticle bandwidth $w$ as functions of $J$. $m_1$ is the effective mass at the $S$ point $\mathbf{k}=(\pi/2,\pi/2)$ in the direction towards the $\Gamma$ point $\mathbf{k}=(0,0)$, $m_2$ that in the direction towards the $M$ point $\mathbf{k}=(0,\pi)$ (see Fig. 6). We have tried to fit power laws to all these quantities without much success, except for $\varepsilon_{\min}$, where we found that

$$\varepsilon_{\min}/t=3.35+2.5(J/t)^{1/2}$$

gives a very good fit between $J=0.01t$ (our lowest value) and $J\sim 0.6t$. This behavior is indicated in Fig. 9(a) (dashed line). An interesting possibility for the $J$ dependence of the quasiparticle spectral weight $z(\pi/2,\pi/2)$ is shown in Fig. 9(b), where we have plotted this quantity versus $J$ (solid circles) and $J^{1/2}$ (asterisks). There is a very good proportionality to $(J/t)^{1/2}$ up to $J\sim 0.7t$, but with negative intercept indicating a different $J$ dependence for very small $J$. In the inset to Fig. 9(b), we show a highly magnified view of the results for very small values of $J$. Here, the quasiparticle residue appears to approach a linear $J$ dependence, as suggested by Kane, Lee, and Read.[4] For large $J$, the quasiparticle residue approaches unity. This can be readily understood by evaluating Eq. (8) perturbatively, using $t/J$ as an expansion parameter.[1] Replacing $G$ in Eq. (8) by the unperturbed hole Green's function $G^0$, one obtains

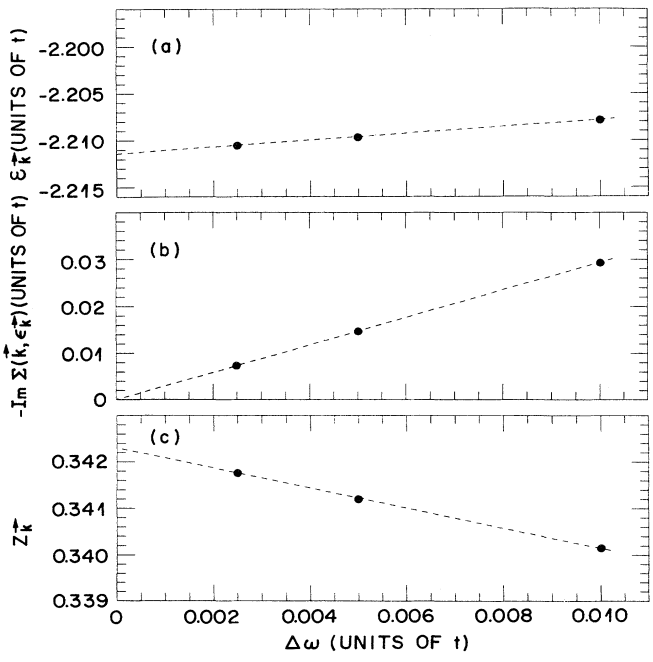


FIG. 8. (a) Quasiparticle energy $\varepsilon_{\mathbf{k}}$, (b) broadening $-\mathrm{Im}\Sigma(\mathbf{k},\varepsilon_{\mathbf{k}})$, and (c) residue $z_{\mathbf{k}}$ vs artificial broadening $\Delta\omega$, for $J=0.2t$ and $\mathbf{k}=(\pi/2,\pi/2)$. All quantities extrapolate in a linear fashion towards their intrinsic values.

$$z_{\mathbf{k}}=\left[1+\frac{t^2z^2}{N}\sum_{\mathbf{q}}\frac{(u_{\mathbf{q}}\gamma_{\mathbf{k}-\mathbf{q}}+v_{\mathbf{q}}\gamma_{\mathbf{k}})^2}{\omega_{\mathbf{q}}^2}\right]^{-1}. \tag{15}$$

Hence, for $J\gg t$, $z_{\mathbf{k}}=1-O(t^2/J^2)$.[1]

For small $J$, the quasiparticle inverse effective masses $m_1^{-1}$ and $m_2^{-1}$ [Fig. 9(c)] and bandwidth $w$ [Fig. 9(d)] display behavior similar to that of $z_{\mathbf{k}}$, i.e., a sublinear rise with $J$. They subsequently go through a maximum at intermediate values of $J$ (between 0.4 and $0.7t$) and decrease again as $J$ increases further. For $J\gg t$ (not shown), one obtains similarly to Eq. (15),

$$\varepsilon_{\mathbf{k}}=-\frac{t^2z^2}{N}\sum_{\mathbf{q}}\frac{(u_{\mathbf{q}}\gamma_{\mathbf{k}-\mathbf{q}}+v_{\mathbf{q}}\gamma_{\mathbf{k}})^2}{\omega_{\mathbf{q}}}, \tag{16}$$

i.e., all quantities vanish as $t^2/J$.[1] The maximum bandwidth occurs near $J=0.4t$ and is of order $t$. The mass anisotropy $m_2/m_1$ varies from 5 to 7 for $0.025t<J<0.9t$, with the maximum occurring near $J=0.15t$.

Kane, Lee, and Read have given arguments that within the noncrossing approximation and for small $J$, the quasiparticle reside $z_{\mathbf{k}}$ and bandwidth $w$ are of order $J/t$ and $J$, respectively.[4] The numerical solution of Eqs. (8) and (9) reveals this behavior to be limited to extremely small values of $J$. For $J>0.025t$, our numerical results for the quasiparticle spectral weight and bandwidth vary sublinearly with $J$.

## V. CONCLUSIONS

We have studied the spectral function of a single hole in a 2D quantum antiferromagnet, using the noncrossing approximation for the hole self-energy proposed earlier in Ref. 1. We have critically examined the validity of this approximation by comparing the results to those of exact diagonalization studies of small systems.[5,6] The agreement is surprisingly good. There are some quantitative discrepancies which presumably arise from our neglect of vertex corrections and the hard-core constraints in the problem. By studying larger systems, we have observed a number of finite-size effects which should also be present in the exact diagonalization results.

The hole spectral function consists of a quasiparticle peak followed by a broad incoherent part. The incoherent part in turn shows some structure, due to multiple spin-wave excitations. With increasing $J$, the quasiparticle residue first increases linearly and then sublinearly from 0 to 1, while the quasiparticle bandwidth first increases and then decreases again, reaching a maximum for $J$ of order $t$.

While the problem of the motion of a single hole in a quantum antiferromagnet is interesting, it is doubtful that it has relevance to the problem of a small, but finite concentration of holes in the thermodynamic limit. As we have seen, for nonzero $J$, the spectral function of a single hole always has a quasiparticle or propagating part, which has led some people to conjecture that for an arbitrarily small concentration of holes, the Heisenberg or large-$U/t$ Hubbard model is a metal, with a Fermi surface determined by filling up the single-hole quasipar-

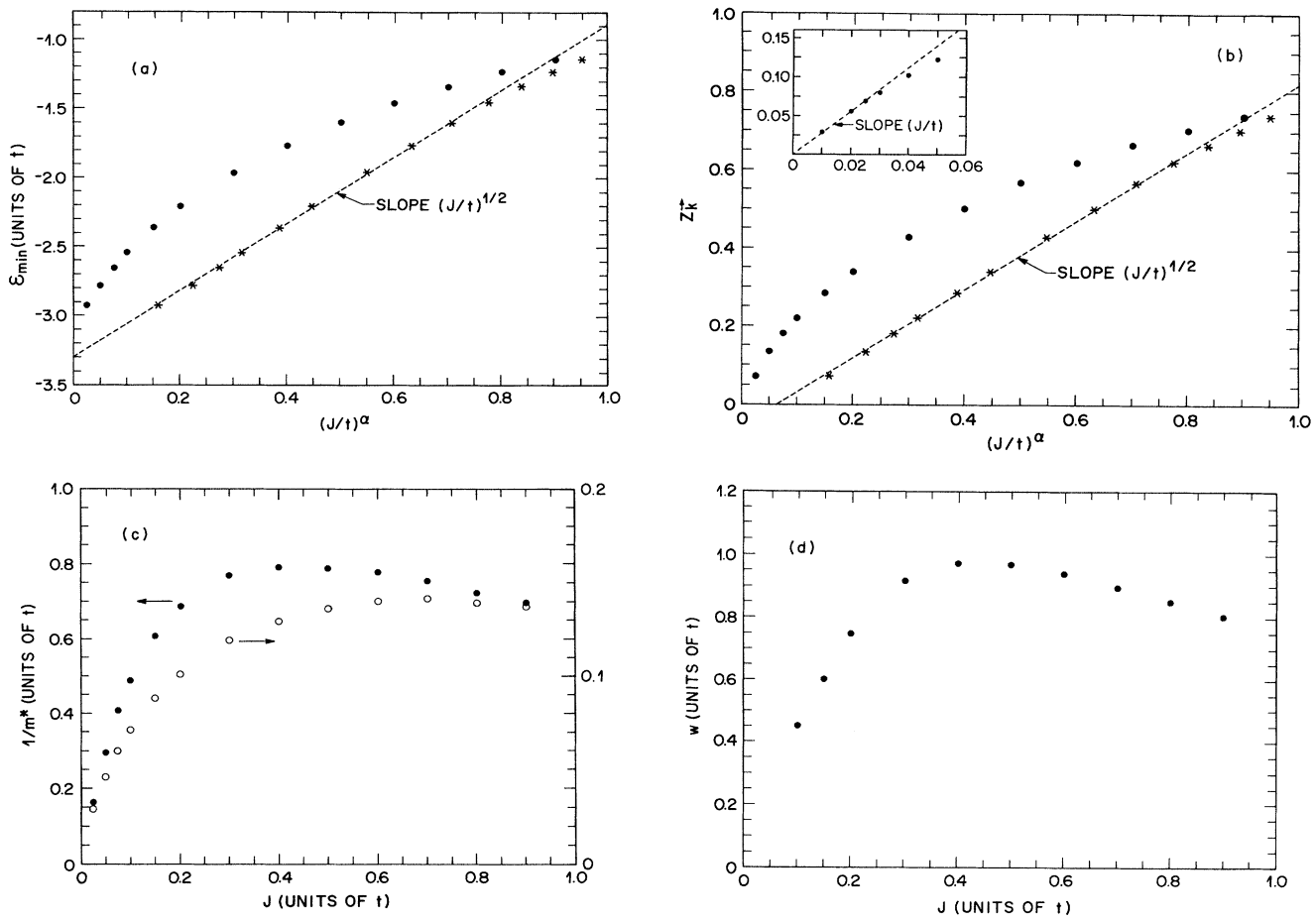


FIG. 9. (a) Hole ground-state energy $\varepsilon_{min}$ vs $J$ (solid circles) and $J^{1/2}$ (asterisks). The dashed line $\varepsilon_{min}/t = -3.35 + 2.5(J/t)^{1/2}$ fits the data up to $J \sim 0.6t$. (b) Quasiparticle residue $z(\pi/2,\pi/2)$ vs $J$ (solid circles) and $J^{1/2}$ (asterisks). The dashed line fits the data up to $J \sim 0.7t$, but has a negative intercept. For very small values of $J$, the dependence appears to be linear, as shown in the inset. (c) Quasiparticle inverse effective masses $m_1^{-1}$ (solid circles, left-hand scale) and $m_2^{-1}$ (open circles, right-hand scale) vs $J$. $m_1$ is the effective mass at $\mathbf{k}=(\pi/2,\pi/2)$ in the direction towards $\mathbf{k}=(0,0)$, $m_2$ that in the direction towards $\mathbf{k}=(0,\pi)$. There is a minimum effective mass at intermediate $J$, and $m_2$ is 5–7 times the value of $m_1$ for $J < t$. (d) Quasiparticle bandwidth $w$ vs $J$. The behavior as a function of $J$ follows that of the inverse effective masses. Results for $J < 0.1t$ are not plotted, because the top of the quasiparticle band becomes ill-defined due to its small spectral weight.

ticle states. In spite of the interesting consequences of this Ansatz,[17] we find this point of view questionable. In fact, recent exact diagonalization studies of the doped Heisenberg model claim that the Fermi surface is always noninteracting-electronlike [i.e., with the minimum in the single-particle dispersion at $\mathbf{k}=(0,0)$].[18] In addition, mean-field studies for $U/t \ll 1$, where well-controlled approximations exist, suggest that for small hole concentrations the ground state might not be a metal at all;[19] rather, the holes generate incommensurate vertical domain walls, the separation of which is determined by the hole concentration. For larger values of the Coulomb repulsion, diagonal domain walls are favored. There have also been speculations that for small hole concentrations the dipolar patterns of spin distortions around a hole will arrange themselves into a metallic spiral order.[20] However, variational states with such spiral order have been shown to be unstable, at least for small and intermediate coupling.[19]

We have learned that identical results for a hole spectral function have also been obtained by Martinez and Horsch.[21]

## ACKNOWLEDGMENTS

We would like to thank Elbio Dagotto and Walter Stephan for providing us with their exact diagonalization results prior to publication and for helpful discussions. The work of F.M. was supported by the Natural Science and Engineering Research Council of Canada and National Science Foundation Grant No. DMR-8918306, and that of A.E.R. by the Sloan Foundation.

*Present address: Theoretical Physics Branch, Chalk River Nuclear Laboratories, Chalk River, ON Canada K0J 1J0.

[1]S. Schmitt-Rink, C. M. Varma, and A. E. Ruckenstein, Phys. Rev. Lett. **60**, 2793 (1988).
[2]W. L. McMillan, Phys. Rev. **175**, 266 (1968).
[3]See, for example, *Polarons and Excitons,* edited by C. G. Kuper and G. D. Whitfield (Plenum, New York, 1963).
[4]C. L. Kane, P. A. Lee, and N. Read, Phys. Rev. B **39**, 6880 (1989).
[5]E. Dagotto, R. Joynt, A. Moreo, S. Bacci, and E. Gagliano, Phys. Rev. B **41**, 9049 (1990).
[6]K. J. von Szczepanski, P. Horsch, W. Stephan, and M. Ziegler, Phys. Rev. B **41**, 2017 (1990).
[7]L. N. Bulaevski, E. L. Nagaev, and D. I. Khomskii, Zh. Eksp. Teor. Fiz. **54**, 1562 (1968) [Sov. Phys. JETP **27**, 836 (1968)].
[8]W. F. Brinkman and T. M. Rice, Phys. Rev. B **2**, 1324 (1970).
[9]B. I Shraiman and E. D. Siggia, Phys. Rev. Lett. **60**, 740 (1988); **61**, 467 (1988).
[10]S. A. Trugman, Phys. Rev. B **37**, 1597 (1988).
[11]S. Sachdev, Phys. Rev. B **39**, 12 232 (1989).
[12]C. Gros and M. D. Johnson, Phys. Rev. B **40**, 9423 (1989).
[13]Z. B. Su, Y. M. Li, W. Y. Lai, and L. Yu, Phys. Rev. Lett. **63**, 1318 (1989).
[14]R. P. Feynmann, Phys. Rev. **94**, 262 (1954); R. P. Feynman and M. Cohen, *ibid.* **102**, 1189 (1956).
[15]R. R. Bartkowski, Phys. Rev. B **5**, 4536 (1972).
[16]Y. Nagaoka, Phys. Rev. **147**, 392 (1966).
[17]S. A. Trugman, Phys. Rev. Lett **65**, 500 (1990).
[18]W. Stephan and P. Horsch (unpublished).
[19]See, for example, H. J. Schulz, Phys. Rev. Lett. **64**, 1445 (1990); M. Inui and P. B. Littlewood (unpublished).
[20]B. I. Shraiman and E. D. Siggia, Phys. Rev. Lett. **62**, 1564 (1989).
[21]G. Martinez and P. Horsch (unpublished).